

Control of two-photon double ionization of helium with intense chirped attosecond laser pulses

S. Barmaki,^{*} P. Lanteigne, and S. Laulan[†]

*Laboratoire de Physique Computationnelle et Photonique, Université de Moncton Campus de Shippagan,
218 Boulevard J. D. Gauthier, Shippagan, New Brunswick E8S 1P6, Canada*

(Received 1 April 2014; published 9 June 2014)

We study the two-photon double-ionization process of the helium atom by solving numerically the nonrelativistic, time-dependent Schrödinger equation in its full dimensionality. We investigate with intense chirped attosecond laser pulses of 23.5-nm wavelength the two-photon absorption near and above the sequential threshold. We show how it is possible by adjusting the chirp parameter to control the electronic transitions inside the atom, thereby reinforcing or weakening the ionization process. Attosecond chirped laser pulses offer a promising way to probe and control the two-photon double ionization of helium when compared with attosecond transform-limited pulses.

DOI: [10.1103/PhysRevA.89.063406](https://doi.org/10.1103/PhysRevA.89.063406)

PACS number(s): 32.80.Rm, 32.80.Fb

I. INTRODUCTION

Many studies have been conducted in past years on the two-photon double ionization (TPDI) of the helium atom, which is the benchmark system for investigating the electronic correlations (see [1–9] and references therein). The majority of studies have focused on the use of a transform-limited laser pulse to trigger the TPDI that could take place as a direct or a sequential ionization process.

In this paper, we used chirped laser pulses instead of transform-limited pulses (unchirped pulses) to investigate the TPDI in helium. The characteristic attribute of chirped laser pulses is their selectivity that has permitted the control of the population transfer in atoms [10–12]. Other recent studies have stressed the efficiency of these pulses to measure attosecond time-scale electron dynamics [13], to extend the cutoff of above-threshold ionization spectra [14], or to induce a red or blue shift of some emitted harmonics [15,16]. We show in the present paper the opportunity that chirped pulses offer to achieve TPDI yield control. To the best of our knowledge, the TPDI by chirped laser pulses in helium has only been addressed by Lee *et al.* [17], where the authors pointed out the sensitivity of the process to the chirp parameter of intense attosecond laser pulses of 13.5-nm wavelength. We report here the first study that demonstrates the efficiency of chirped laser pulses to control the transfer of the population to the double-continuum electronic states, thereby reinforcing or, conversely, weakening the ionization process.

We numerically investigate the TPDI process in helium under intense chirped attosecond laser pulses of 23.5-nm wavelength, which corresponds to the 34th harmonic of an 800-nm wavelength Ti-sapphire laser. Our time-independent theoretical approach to calculate the whole atomic spectrum is based on a discretization technique using B-spline functions [18,19]. The approach we used to solve the time-dependent Schrödinger equation is based on a spectral method of configuration interaction type that gives very accurate results and incorporates electron-electron correlations with a high degree of accuracy [3]. At the end of the laser-atom interaction, we extract the population of the doubly ionized states

by projecting the total electronic wave function onto Coulomb states. After that, the calculation of physical quantities necessary to analyze the behavior of the two active electrons under a chirped pulse, such as the total two-photon double-ionization probability and the energy distribution of ejected electrons, is straightforward. We determine the effect of the sign and the magnitude of the chirp parameter on these quantities. In contrast with transform-limited pulses, chirped laser pulses are of time-dependent frequency. The latter increases or decreases with time depending on the sign of the chirp, which offers the possibility to control the electronic transitions inside the atom. The amount of the population transferred to the double continuum can then be enhanced or decreased, enabling us to achieve a double-ionization yield control.

Atomic units ($m_e = \hbar = e = 1$) are used throughout the paper unless otherwise stated.

II. THEORETICAL APPROACH

A. Atomic structure calculations

The full electronic eigenvalue problem, i.e., the time-independent Schrödinger equation (TISE) for the helium atom, is given by

$$H\psi_n^{L,M}(\mathbf{r}_1, \mathbf{r}_2) = E_n\psi_n^{L,M}(\mathbf{r}_1, \mathbf{r}_2). \quad (1)$$

The nonrelativistic Hamiltonian H reads as follows:

$$H = -\frac{1}{2}\Delta_1 - \frac{1}{2}\Delta_2 - \frac{Z}{r_1} - \frac{Z}{r_2} + \frac{1}{|\mathbf{r}_1 - \mathbf{r}_2|}, \quad (2)$$

where r_1 and r_2 are the distances from the nucleus of charge $Z = 2$ to electrons 1 and 2, respectively. For a given total angular momentum L and projection M , the stationary wave function $\psi_n^{L,M}(\mathbf{r}_1, \mathbf{r}_2)$ is expanded on a basis of two-electron configurations that are products of one-electron functions as follows:

$$\psi_n^{L,M}(\mathbf{r}_1, \mathbf{r}_2) = \mathcal{A} \sum_{\alpha=i,j,l_1,l_2} c_{n,\alpha}^{L,M} \frac{B_i^k(r_1)}{r_1} \frac{B_j^k(r_2)}{r_2} \mathcal{Y}_{l_1,l_2}^{L,M}(1,2), \quad (3)$$

where \mathcal{A} is the antisymmetrization operator, and $l_1(l_2)$ is the angular momentum of electron 1(2). The angular part of $\psi_n^{L,M}(\mathbf{r}_1, \mathbf{r}_2)$ is described by the bipolar spherical harmonic function $\mathcal{Y}_{l_1,l_2}^{L,M}(1,2)$, while the radial part is interpolated by

^{*}samira.barmaki@umoncton.ca

[†]stephane.laulan@umoncton.ca

a product of B-spline functions of order k [18,19]. The N_b B-spline function basis set is defined on the radial interval (box) $I = [0, R_{\max}]$. Each i th B-spline $B_i^k(r)$ of this set is composed of polynomial pieces of degree $k - 1$ and is only nonzero in a well-defined limited radial segment of I . With this interesting property, there are no large cancellations between contributions of the various B-spline functions, which insures the numerical stability. By substituting Eq. (3) in Eq. (1) and by projecting on every B-spline product, the TISE is reduced to a system of linear equations that can be written in the matrix form as $HC = ESC$. The resulting Hamiltonian matrix H and the positive overlap matrix S are symmetric and banded. The straightforward diagonalization of Eq. (1) gives the eigenenergies E_n and the expansion coefficients $c_{n,\alpha}^{L,M}$ of all bound and continuum electronic states. More details about the application of B-spline functions in the calculation of the unperturbed electronic structure of two- and three-electron atomic systems are given in [4–6] and references therein.

B. Time-dependent calculations

Within the electric dipole approximation, the time-dependent Schrödinger equation (TDSE) is given, in the velocity gauge, by

$$i \frac{\partial}{\partial t} \Psi(\mathbf{r}_1, \mathbf{r}_2, t) = [H + (\mathbf{p}_1 + \mathbf{p}_2) \cdot \mathbf{A}(t, \xi)] \Psi(\mathbf{r}_1, \mathbf{r}_2, t). \quad (4)$$

The chirped laser pulse is assumed to be polarized along the z axis, with its vector potential given by

$$\mathbf{A}(t, \xi) = A_0 f(t) \sin[\omega(t, \xi)t] \mathbf{e}_z, \quad (5)$$

with ξ as the dimensionless chirp parameter. A_0 is the peak amplitude, which is related to the laser pulse central frequency ω_0 and the peak intensity I_0 by

$$A_0 = \frac{1}{\omega_0} \sqrt{\frac{I_0}{I_{\text{a.u.}}}}, \quad (6)$$

where $I_{\text{a.u.}} = 3.51 \times 10^{15} \text{ W/cm}^2$ is the atomic unit of intensity. We consider the laser pulse having a Gaussian time envelope $f(t)$ identical to that given in [17,20]:

$$f(t) = \exp \left[-2 \ln 2 \frac{t^2}{\tau_0^2} \right]. \quad (7)$$

We note that the chirp filters used in laser pulse generation techniques are implemented by means of dispersive optical systems. Upon transmission through a filter characterized by a b chirp coefficient, an initially transform-limited pulse ($\xi = 0$) becomes chirped, i.e., with frequency $\omega(t, \xi)$ that varies in time and depends on the chirp parameter $\xi = b/\tau_0^2$. (For the experimental details, see [20].) τ_0 is the FWHM duration of the transform-limited pulse. The generated pulse is said to be up-chirped if ξ is positive and down-chirped if ξ is negative [20]. Its instantaneous frequency $\omega(t, \xi)$ and its frequency bandwidth $\Delta\omega$ are given, respectively, by

$$\omega(t, \xi) = \omega_0 + 4 \ln 2 \frac{\xi t}{\tau_0^2}, \quad (8)$$

$$\Delta\omega = \frac{4 \ln 2 \sqrt{1 + \xi^2}}{\tau_0}. \quad (9)$$

The time-dependent total wave function is expanded on the basis of the field-free atomic eigenstates, normalized to unity:

$$\Psi(\mathbf{r}_1, \mathbf{r}_2, t) = \sum_{\alpha \equiv n, L}^{N_s, L_{\max}} C_\alpha(t) \psi_n^{L, M}(\mathbf{r}_1, \mathbf{r}_2). \quad (10)$$

By substituting Eq. (10) into Eq. (4), we obtain a set of coupled integro-differential equations, which we solved using an explicit fifth-order Runge-Kutta numerical method. Electron-electron correlations are included during the integration of the TDSE over the total pulse duration. The helium atom He is considered to be, before its exposure to the pulse, in its electronic ground state $1s^2$, which sets the following initial condition:

$$\Psi(\mathbf{r}_1, \mathbf{r}_2, t_{\text{initial}}) = \psi_{1s^2}^{L, M=0}(\mathbf{r}_1, \mathbf{r}_2). \quad (11)$$

The linear polarization of the laser field implies that only electronic transitions between states of $\Delta M = 0$ are permitted. Hence it is assumed in the following that $M = 0$.

At the end of the laser pulse, the population of a given stationary state $\psi_{k_1 l_1 k_2 l_2}^L(\mathbf{r}_1, \mathbf{r}_2)$ in the atomic double continuum can be obtained by projecting this state on the total wave function:

$$P^L(E_{k_1 l_1}, E_{k_2 l_2}) = \left| \langle \psi_{k_1 l_1 k_2 l_2}^L(\mathbf{r}_1, \mathbf{r}_2) | \Psi(\mathbf{r}_1, \mathbf{r}_2, t_{\text{final}}) \rangle \right|^2, \quad (12)$$

where $E_{k_i l_i}$ is the energy of the $k_i l_i$ electron. We neglect, in our calculations of $P^L(E_{k_1 l_1}, E_{k_2 l_2})$, the electron-electron correlations in the double-continuum state $\psi_{k_1 l_1 k_2 l_2}^L(\mathbf{r}_1, \mathbf{r}_2)$, which we approximate by a simple antisymmetrized product of hydrogenic functions $\phi_{kl}(\mathbf{r}) = R_{kl}(r) Y_l^m(\theta, \phi)$. We note that this approximation has proven its efficiency to correctly describe the general shape of the electron energy distribution resulting from the two-photon double-ionization process [3]. In this case, the double-continuum wave function $\psi_{k_1 l_1 k_2 l_2}^L(\mathbf{r}_1, \mathbf{r}_2)$ simply reads

$$\psi_{k_1 l_1 k_2 l_2}^L(\mathbf{r}_1, \mathbf{r}_2) = \mathcal{A} [R_{k_1 l_1}(r_1) R_{k_2 l_2}(r_2) \mathcal{Y}_{l_1, l_2}^{L, M}(1, 2)], \quad (13)$$

with

$$\langle \psi_{k_1 l_1 k_2 l_2}^L(\mathbf{r}_1, \mathbf{r}_2) | \psi_{k_1 l_1 k_2 l_2}^L(\mathbf{r}_1, \mathbf{r}_2) \rangle = 1 \quad (14)$$

and

$$\left[-\frac{1}{2} \Delta_i - \frac{Z}{r_i} - E_{k_i l_i} \right] \phi_{k_i l_i}(\mathbf{r}_i) |_{i=1,2} = 0. \quad (15)$$

The radial part of Eq. (15) is solved by interpolating $R_{k_i l_i}(r_i)$ with the same B-spline function basis set used to solve Eq. (1).

C. Physical quantities of interest

The last step of the calculations consists of extracting the following three physical quantities necessary to analyze the effect of an intense chirped laser pulse on the helium atom. The first quantity is the total two-photon double-ionization ($2\omega, 2e$) probability that can simply be obtained by summing the contributions of the ($L = 0, l_1, l_2$) and ($L = 2, l_1, l_2$) channels:

$$P(2\omega, 2e) = \sum_{(L=0,2, k_1 l_1, k_2 l_2)} P^L(E_{k_1 l_1}, E_{k_2 l_2}). \quad (16)$$

The second quantity is the electron energy distribution of both ejected electrons of energy $E_{k_1 l_1}$ and $E_{k_2 l_2}$, which can

be extracted as follows:

$$\frac{d^2 P^L(E_{k_1 l_1}, E_{k_2 l_2})}{dE_{k_1 l_1} dE_{k_2 l_2}} = \rho(E_{k_1 l_1}) \rho(E_{k_2 l_2}) P^L(E_{k_1 l_1}, E_{k_2 l_2}), \quad (17)$$

where $\rho(E_{k_i l_i})$ is the density of states in the $k_i l_i$ continuum [3,18]. And finally, the third is the distribution of a single ejected electron of energy $E_{k_1 l_1}$ in the atomic double continuum that can readily be calculated as follows:

$$\frac{dP^L(E_{k_1 l_1})}{dE_{k_1 l_1}} = \sum_{E_{k_2 l_2}} \rho(E_{k_1 l_1}) P^L(E_{k_1 l_1}, E_{k_2 l_2}). \quad (18)$$

III. RESULTS AND DISCUSSION

We consider in our calculations a set of $N_b = 50$ B-splines of order $k = 7$ defined on the radial box $[0, R_{\max} = 50]$ atomic units (a.u.). We expand the stationary electronic wave function [see Eq. (3)] on a basis of (L, l_1, l_2) combination terms, where the l_1 and l_2 angular momenta ($0 \leq l_1, l_2 \leq 3$) couple to total angular momentum $0 \leq L \leq 3$. The convergence of our numerical results has been checked by increasing the number of B-splines, the radial box size, and the number of angular momenta. We also checked that the results of the numerical integration of TDSE are gauge independent.

Before we present our study of the TPDI process by a chirped laser pulse of time-dependent frequency, we recall, as indicated in Fig. 1, how the process takes place as a direct or a sequential process under a laser pulse of constant frequency ω_0 [3–6]. In order to overcome the He($1s^2$) double-ionization potential of 2.903 a.u. (79 eV), ω_0 has to be higher than 1.45 a.u. Direct ionization is the only energetically possible process to take place if ω_0 is insufficiently high to overcome the He⁺($1s$) ionization potential of 2 a.u.; the ejected electrons in this case share uniformly the excess energy $E_{ex} = -2.903 + 2\omega_0$ a.u. [1]. For ω_0 larger than 2 a.u., both processes take place but the sequential one will be dominant. The electron energy distribution exhibits in this case two peaks: one located at $E_1 = E_{He(1s^2)} + \omega_0 - E_{He^+(1s)}$ a.u., which is

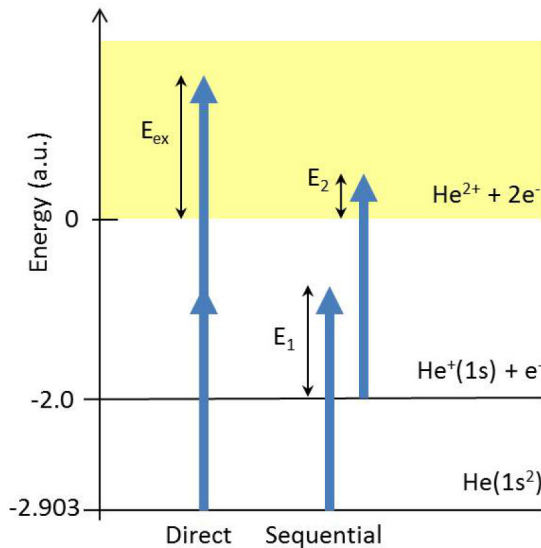


FIG. 1. (Color online) Schematic He energy-level diagram showing the direct and the sequential ionization processes from $1s^2$.

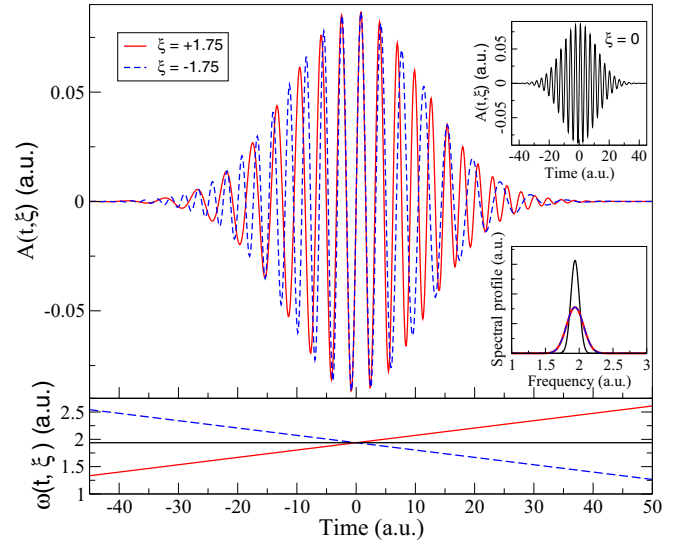


FIG. 2. (Color online) Dependence of laser pulse vector potential $A(t, \xi)$, spectral profile, and instantaneous frequency $\omega(t, \xi)$ on the chirp parameter ξ for three cases $\xi = 0, \pm 1.75$. Each laser pulse has a central frequency $\omega_0 = 1.938$ a.u. (52.7 eV), peak intensity 10^{15} W/cm², and FWHM duration $\tau_0 = 460$ asec.

the energy of the ejected electron after the absorption of the first photon by He; and the second located at lower energy $E_2 = E_{He^+(1s)} + \omega_0$ a.u., resulting from the ionization of the He⁺ by the absorption of the second photon.

In our investigation, we trigger the TPDI process by exposing the atom to a laser pulse [see Eq. (5)] of 23.5-nm wavelength ($\omega_0 = 1.938$ a.u.), a peak intensity of 10^{15} W/cm², and a FWHM duration of $\tau_0 = 460$ asec. Figure 2 depicts the dependence of laser pulse vector potential $A(t, \xi)$, spectral profile, and instantaneous frequency $\omega(t, \xi)$ on the chirp parameter ξ , as shown, for example, for $\xi = 0, \pm 1.75$. For $\xi = 0$, the laser pulse is a transform-limited pulse that keeps its frequency constant with time, in contrast with an up-chirped (down-chirped) pulse with a positive (negative) value of ξ that sees its instantaneous laser frequency increases (decreases) with time. We present in Fig. 3 the total atomic

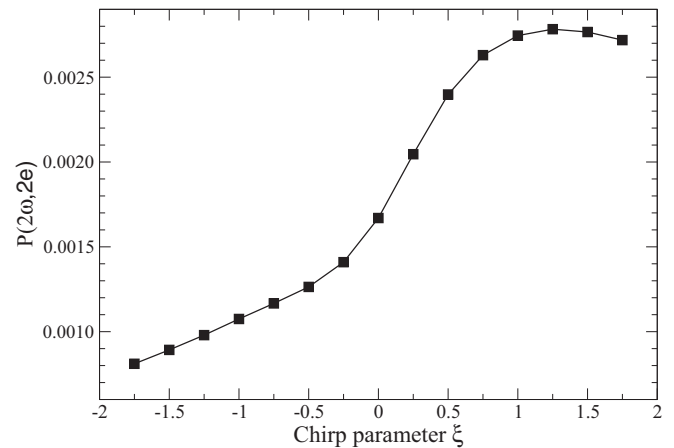


FIG. 3. Total two-photon double-ionization probability $P(2\omega, 2e)$ as a function of the chirp parameter ξ .

two-photon double-ionization probability $P(2\omega, 2e)$ obtained with Eq. (16) by the transform-limited pulse and chirped laser pulses of ξ values ranging from -1.75 to $+1.75$. Figure 3 clearly indicates the sensitivity of the TPDI process to the sign of ξ . The discrepancy between the $P(2\omega, 2e)$ obtained for each positive and negative ξ becomes increasingly pronounced by strengthening the chirp. An up-chirped laser pulse, in contrast with a down-chirped laser pulse of the same peak intensity and the same chirp magnitude $|\xi|$ (the same frequency bandwidth), clearly boosts the ionization process. With an up-chirped laser pulse of a strengthened chirp of $\xi = +1.75$, the $P(2\omega, 2e)$ is more than 3 times higher than with $\xi = -1.75$, as depicted in Fig. 3. The right adjustment of the chirp parameter, as demonstrated by the results, could be indeed an effective means for achieving TPDI yield control in the He atom.

The sensitivity of $P(2\omega, 2e)$ to the chirp parameter results directly from the time and the chirp dependence of the instantaneous frequency $\omega(t, \xi)$. As we can see in the insert of Fig. 2, the $\omega(t, \xi)$ of a chirped laser pulse varies differently in time, depending on the sign of the chirp. In this case, the frequency of the second absorbed photon by the atom will differ from that of the first photon, which will dictate whether the TPDI will be reinforced or weakened. For a better understanding of how the chirp has an effect on the TPDI process, we looked at the results of the electron energy distribution of both ejected electrons of energy E_1 and E_2 and the single electron energy distribution [see Eqs. (17) and (18)] of the He atom exposed to the transform-limited pulse ($\xi = 0$) and the up- and down-chirped laser pulses used before. Figure 4 shows the results obtained in the dominant channel ($L = 2, l_1 = 1, l_2 = 1$) when $\xi = 0$ and $\xi = \pm 1.75$. The TPDI process by the transform-limited pulse is expected to occur in the “far” direct regime near the region of the sequential ionization threshold, as the absorbed photons have in this case the constant frequency of $\omega_0 = 1.938$ a.u., which is close to the He⁺ ionization threshold of 2 a.u. The electrons exposed to such laser frequency do not have to interact strongly in order to overcome the attraction of the nucleus; hence the sequential process takes over the direct one, as it is clearly indicated in Fig. 4(a). Here, a first absorbed photon ejects one of the two electrons, creating the residual He⁺ ion that immediately relaxes into its ground state $1s$. Although, in this particular case, a second photon does initiate the second step of the sequential process, it is of insufficient energy to eject the electron of He⁺ well beyond the He double-ionization threshold, which results rather in populating the He⁺ Rydberg states and less the double-continuum electronic states. Figure 4(a) shows that the single electron energy distribution exhibits, in this case, two maxima at the edges (U-shaped structure); the first ionized electron absorbs most of the interaction energy, $\langle 1s^2 | \frac{1}{|r_1 - r_2|} | 1s^2 \rangle$, which is converted into kinetic energy, while a minimum is transferred to the other electron. With any of the down-chirped laser pulses we used, we observed that the sequential two-photon absorption still holds. However, the TPDI process is considerably weakened compared to when the atom is under the transform-limited pulse. In this case, as the $\omega(t, \xi)$ of a down-chirped pulse decreases linearly with time and gets lower than ω_0 in the second half of its duration, the absorption of the second photon enhances the population of the He⁺ excited states,

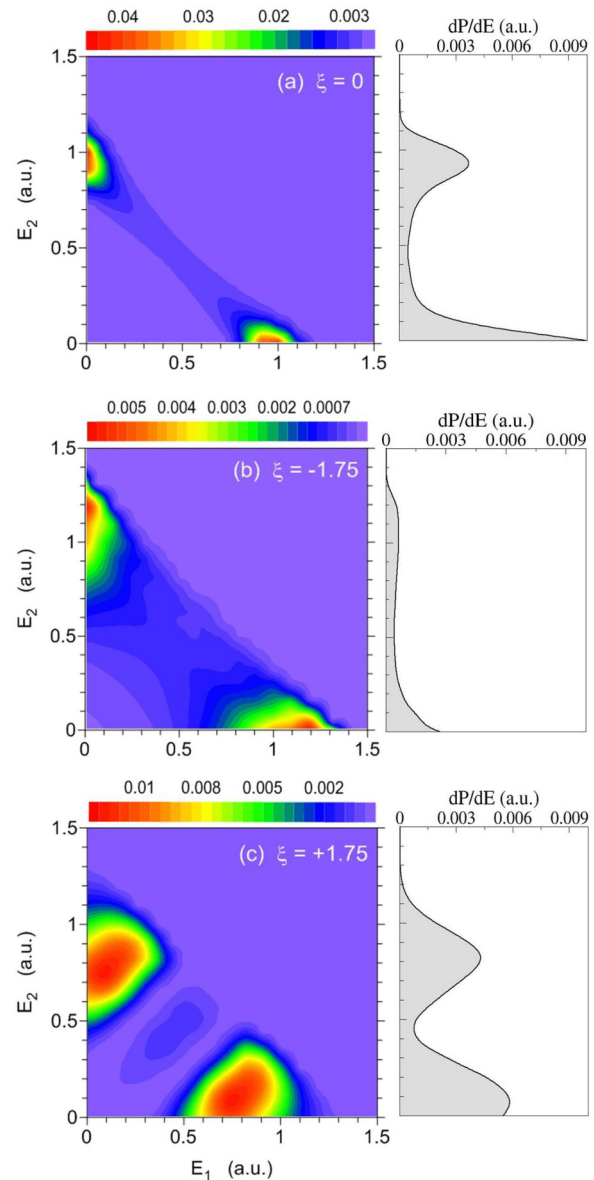


FIG. 4. (Color online) (Right) Single electron energy distribution (dP/dE) as a function of ejected electron energy. (Left) Contour plots of the electron energy distribution of both ejected electrons of energies E_1, E_2 in the dominant channel ($L = 2, l_1 = 1, l_2 = 1$) for $\xi = 0$ and ± 1.75 .

which weakens the double-ionization yield far more than in the previously studied case. The general shape of the electron energy distribution for all negative ξ , as is shown, for example, in Fig. 4(b) for $\xi = -1.75$, is of a flattened structure. The results indicate that the double continuum is much less populated here, which explains the decrease of $P(2\omega, 2e)$ when He is exposed to down-chirped pulses compared to when it is under the transform-limited pulse (see Fig. 3). In the above studies, the sequential two-photon absorption is dominant, as each electron absorbs a photon and attempts to escape independently from the other, which causes an unequal energy sharing between them. However, the control of the repartition of the energy between the ejected electrons by a down-chirped laser pulse could be possible by adequately adjusting its chirp

magnitude $|\xi|$. The more we strengthen the latter, the more we make $\omega(t, \xi)$ increasingly lower than ω_0 . With $|\xi| \gg 1.75$, we can reach the “deep” direct regime, $1.45 \ll \omega(t, \xi) \leq 1.65$; the TPDI process will then take place mainly as a direct process. The electrons that will strongly interact in this case to overcome the attraction of the nucleus will be ejected almost simultaneously, sharing the excess energy uniformly.

The response of the atom to an up-chirped laser pulse of $+\xi$ of the same peak intensity and spectral width than a down-chirped pulse of $-\xi$ is quite different. We observe in Fig. 4(c) that for $\xi = +1.75$, the electron energy distribution reaches its maximum at two distinguished peaked areas separated by a deep valley. Under an up-chirped laser pulse, one electron takes the majority of the available energy via the ionization of He($1s^2$) by the absorption of the first photon. The instantaneous frequency $\omega(t, \xi)$, in this case, keeps increasing as the pulse progresses. By strengthening the chirp, the frequency reaches values $\omega(t, \xi) \geq 2$ a.u. at the beginning of the second half duration of the pulse, which makes the second absorbed photon acquire enough energy to eject the other electron beyond the He ionization threshold, thus populating the double-continuum states much more. In contrast with a down-chirped pulse, the TPDI process is here clearly reinforced, which explains the significant increase of $P(2\omega, 2e)$ when the atom is under up-chirped pulses (see Fig. 3).

IV. CONCLUSION

We have investigated the interaction of the two active electrons of the helium atom with chirped attosecond laser pulses of 23.5-nm wavelength and an intensity of 10^{15} W/cm². The electronic correlations have been included in

the initial ground state and during the numerical solution of the time-dependent Schrödinger equation. We have projected, at the end of the laser pulse, the total electronic wave function onto double-continuum states in order to extract the physical quantities of interest. The double continuum has been approximated by an antisymmetrized product of hydrogenic functions. We have analyzed the effect of the sign and the magnitude of the chirp on the two-photon double-ionization probability and the energy distributions of ejected electrons. The findings of the presented study have demonstrated that chirped laser pulses are promising tools that offer the possibility to achieve a two-photon double-ionization yield control. Instead of transform-limited pulses, chirped laser pulses are of time-dependent frequency that depends on the chirp parameter. The appropriate adjustment of the latter is the key to successfully achieve the control of the way the two active electrons will leave the atom and how much energy each will acquire. Our numerical study could easily be applicable to any multielectron atom having two valence electrons. We will assume in this case that the laser field will not influence the core electrons. We hope that the findings of this study will guide future experiments on the control of atomic ionization by chirped attosecond laser pulses.

ACKNOWLEDGMENTS

The present research was supported by the Nature Sciences and Engineering Research Council (NSERC) and by the New Brunswick Innovation Foundation (NBIF). Allocation of CPU time and assistance with the computer facilities from Compute Canada are acknowledged.

-
- [1] H. Bachau, *Phys. Rev. A* **83**, 033403 (2011).
 - [2] R. Pazourek, J. Feist, S. Nagele, E. Persson, B. I. Schneider, L. A. Collins, and J. Burgdörfer, *Phys. Rev. A* **83**, 053418 (2011).
 - [3] S. Laulan and H. Bachau, *Phys. Rev. A* **68**, 013409 (2003).
 - [4] B. Piraux, J. Bauer, S. Laulan, and H. Bachau, *Eur. Phys. J. D* **26**, 7 (2003).
 - [5] E. Fomouuo, S. Laulan, B. Piraux, and H. Bachau, *J. Phys. B: At., Mol. Opt. Phys.* **39**, S427 (2006).
 - [6] S. Laulan and H. Bachau, *Phys. Rev. A* **69**, 033408 (2004).
 - [7] H. Hasegawa, E. J. Takahashi, Y. Nabekawa, K. L. Ishikawa, and K. Midorikawa, *Phys. Rev. A* **71**, 023407 (2005).
 - [8] A. A. Sorokin, M. Wellhofer, S. V. Bobashev, K. Tiedtke, and M. Richter, *Phys. Rev. A* **75**, 051402 (2007).
 - [9] M. Kurka, J. Feist, D. A. Horner, A. Rudenko, Y. H. Jiang, K. U. Kühnel, L. Foucar, T. N. Rescigno, C. W. McCurdy, R. Pazourek *et al.*, *New J. Phys.* **12**, 073035 (2010).
 - [10] S. Laulan, J. Haché, H. S. Ba, and S. Barmaki, *J. Mod. Phys.* **4**, 20 (2013).
 - [11] S. Laulan, H. S. Ba, and S. Barmaki, *Can. J. Phys.* **92**, 194 (2014).
 - [12] K. J. Schafer and K. C. Kulander, *Laser Phys.* **7**, 740 (1997).
 - [13] G. L. Yudin, A. D. Bandrauk, and P. B. Corkum, *Phys. Rev. Lett.* **96**, 063002 (2006).
 - [14] T. Nakajima, *Phys. Rev. A* **75**, 053409 (2007).
 - [15] X.-B. Bian and A. D. Bandrauk, *Phys. Rev. A* **83**, 041403 (2011).
 - [16] C. A. Popovici, R. A. Ganeev, F. Vidal, and T. Ozaki, *J. Phys. B: At., Mol. Opt. Phys.* **45**, 035601 (2012).
 - [17] T. G. Lee, M. S. Pindzola, and F. Robicheaux, *Phys. Rev. A* **79**, 053420 (2009).
 - [18] H. Bachau, E. Cormier, P. Decleva, J. E. Hansen, and F. Martin, *Rep. Prog. Phys.* **64**, 1815 (2001).
 - [19] C. de Boor, *A Practical Guide to Splines* (Springer, New York, 1978).
 - [20] B. E. A. Saleh and M. C. Teich, *Fundamentals of Photonics* (John Wiley and Sons, Inc., New York, 2007).